Monolithic Fiber Lasers Combining Active PCF With Bragg Gratings in Conventional Single-Mode Fibers

Clémence Jollivet, Julie Guer, Peter Hofmann, and Axel Schülzgen

***Abstract*—Novel monolithic fiber laser architectures utilizing large mode area (LMA) photonic crystal fiber (PCF) and fiber Bragg gratings (FBG) in conventional single-mode fibers (SMF) are presented. The main challenge is to address high cavity losses arising from the intrinsic 18-fold mode-field mismatch between the SMF and the active LMA PCF. Employing an all-fiber, robust and reproducible mode-field matching approach based on graded-index multimode fibers, we numerically and experimentally demonstrate that the SMF-to-LMA PCF coupling can be more than three-fold improved. This MFA approach is further implemented in monolithic fiber laser cavities combining FBGs in SMF and active LMA PCF. We demonstrate that cavity losses can be significantly mitigated when using appropriate MFAs resulting in a substantial increase of the laser output performances.**

***Index Terms*—Optical fiber devices, optical fiber lasers.**

I. Introduction

DURING the past decade, many applications have benefitted from the development of novel designs of specialty fibers. In particular, increased performances of fiber lasers in terms of power and energy scaling have been reported [1], [2], first employing large-mode area (LMA) step-index fibers (SIF) [3] and later using LMA photonic crystal fibers (PCF) [4]. In the meantime, the number and diversity of fiber-based optical devices commercially available keep increasing, offering many design possibilities for all-fiber laser cavities. Monolithic fiber lasers present several advantages over systems based on free space elements: they are more compact, alignment-free, and most importantly stable laser emission is therefore easier to achieve. To date, several LMA SIF-based high power laser systems presenting monolithic architectures have been demonstrated [5], [6]. However, LMA PCF-based laser and amplifier systems typically employ several free space sections, occupying large footprints and requiring complex and sensitive alignment procedures which strongly influence the laser output stability, performances and handling [7]–[9].

Manuscript received November 19, 2013; revised December 6, 2013; accepted December 19, 2013.

C. Jollivet, P. Hofmann, and A. Schülzgen are with the CREOL, College of Optics and photonics, University of Central Florida, Orlando, FL 32816 USA (e-mail: jollivet@creol.ucf.edu; phofmann@creol.ucf.edu; axel@creol.ucf.edu).

J. Guer is with the Department of Physics, Université of Bordeaux 1, Talence 33405, France (e-mail: julieguer@gmail.com).

Color versions of one or more of the figures in this paper are available online at http://ieeexplore.ieee.org.

Digital Object Identifier 10.1109/JSTQE.2013.2296745

The monolithic integration of LMA PCFs is attractive and yet challenging due to the poor compatibility with single-mode fiber (SMF) -based components. First of all, the complex nature of the inner structure of PCFs requires highly controlled splicing procedures to achieve low-loss SMF-PCF splices. Thus, detrimental effects such as air-holes collapsing, stress formation at the splice and misalignment need to be mitigated. In the case where the SMF and the PCF present similar mode-field diameters (MFD), successful splices have been realized using controlled fusion splicing techniques [10]–[13] and CO_2 lasers [14]. Efficient light transmission with splice losses between $\sim$0.5 up to $\sim$2 dB/splice has been measured. On the other hand, PCF core dimensions, in particular LMA designs, differ from typical SMF. As a result of the mode-field mismatch, the PCF-to-SMF coupling exhibits substantial losses. At a specific wavelength where both LMA PCF and SMF operate single-mode, the transmission can be calculated [15]:

$$T = \frac{4\omega_1^2\omega_2^2}{\left(\omega_1^2 + \omega_2^2\right)^2} \tag{1}$$

with ω_1 and ω_2 the two modal-field radii of the optical fibers. Coupling between small PCF and SMF has been demonstrated using mode-field matching techniques involving tapering [16], [17] and pressure-assisted splicing [18]. In addition, a few mode-field matching techniques have been reported between large PCF-to-SMF. One of them involved a GRIN fiber lens surrounded by two coreless fiber segments to reproduce the typical scheme of free-space imaging [19]. However, this approach is limited to passive PCFs with a maximum PCF-to-SMF mode-field- mismatch on the order of four. Furthermore, thermal expansion of cores is a method commonly employed in industry to efficiently couple pump light from multi-mode SIF into double cladding LMA PCF-based high power fiber amplifiers [20]. This method follows several highly controlled steps and requires a rather heavy and expensive piece of equipment. Thus, mode-matching methods involve highly controlled multi-steps procedures where the inner structure and size of the PCF are permanently modified. In addition, the guiding properties of light in the fiber core are changed according to the overall fiber deformation which can substantially influence the output performances of the system.

In order to assemble a monolithic LMA PCF-based laser cavity, one could directly inscribe fiber Bragg gratings (FBG) in the active PCF [21]. However, this technique has not been employed with LMA PCF to date and efficiently coupling the

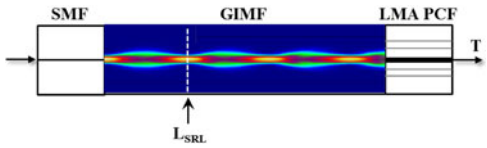

Fig. 1. Schematic representation of a typical all-fiber mode-field adapter (MFA) device using a graded-index multimode fiber (GIMF). The case of mode-field matching between SMF-to-LMA PCF is illustrated. The self-reproduction length (SRL) is indicated by the arrow.

generated laser emission with conventional fiber-based components remains and entire challenge.

Here, we employ a recently demonstrated non-destructive, all-fiber, mode-field matching approach [22], [23]. We demonstrate that the initial eighteen-fold core mode-field mismatch between a LMA PCF and a conventional SMF can be greatly reduced leading to a significant improvement of light transmission. As a result, we demonstrate monolithic fiber lasers employing all-fiber MFAs to combine an active LMA PCF and conventional FBGs in SMF.

II. All-Fiber Mode-Field Adapters

The mode-field matching approach is based on multimode interference (MMI) in graded-index multi-mode fibers (GIMF) [22], [23]. All-fiber MFA devices use a selected piece of graded index multi-mode fiber (GIMF) spliced to two mode mismatched fibers. As an example, a SMF-to-PCF MFA device is schematically represented in Fig. 1. The periodic intensity pattern illustrated in the GIMF section (see Fig. 1) represents the MMI during light propagation in the core of the GIMF. Compared to other multi-mode fibers, GIMFs offer the particularity of guiding multiple transverse modes with evenly spaced effective indices.

The resulting MMI is periodic. At the self-reproduction length (SRL), labeled L_{SRL} and highlighted in Fig. 1, all guided modes constructively interfere and the input field is reproduced. At half the SRL, guided modes destructively interfere and the GIMF acts like a beam expander [22].

Thus, by adjusting the GIMF length and the light wavelength, a wide range of modal-field can be matched. The performances of these all-fiber MFA devices have been experimentally investigated as function of wavelength and temperature [23]. It has been demonstrated that mode-field matching can be achieved across large bandwidth (hundreds of nm) when using short-length devices. Such MFAs are also temperature-independent below 100 °C which make them particularly attractive to mode-match LMA PCF and SMF.

III. Numerical Approach

Our fiber laser experiments utilize a double-clad Yb-doped LMA PCF presenting a 30 μm MFD at 1064 nm, 40 μm core in diameter ($\sim$0.07 NA) and a 200 μm pump cladding diameter (NA $>$ 0.5). This fiber, commercial product by NKTphotonics, has already been implemented in free-space based laser and amplifier systems.

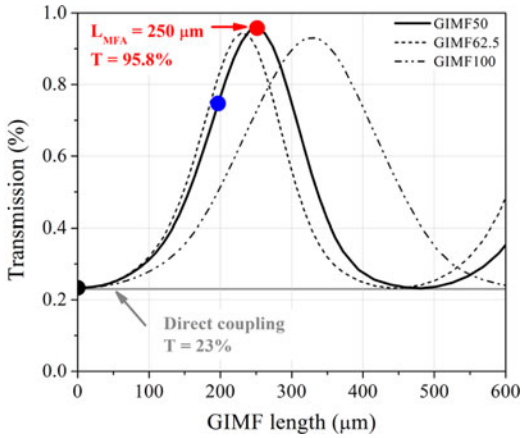

Fig. 2. Numerical simulation of the transmission as function of GIMF length. Three chains employing three different GIMFs are investigated. The red, blue, and black markers refer to laser chains characterized in Fig. 9.

The conventional SMF (SM980 from Fibercore with 5.8 μm core diameter and $\sim$0.12 NA) containing the FBGs has a single-mode cutoff at approximately 980 nm wavelength and an MFD of 6.3 μm at 1064 nm wavelength. As a result, the LMA PCF and SMF present an intrinsic eighteen-fold mode-field mismatch. According to (1), when light is directly coupled from the SMF into the LMA PCF, the corresponding transmission is predicted around $\sim$23% due to the mode-field mismatch.

In this section, we present results from numerical simulations that have been performed using Fimmwave, a commercial software package (by PhotonDesign). Several GIMF-based MFAs configurations are investigated to mitigate the coupling losses between the SMF and the LMA PCF. Light transmission at 1064 nm wavelength through the fiber chain SMF-GIMF-PCF presented in Fig. 1 has been calculated as a function of the length of the GIMF segment. Results are plotted in Fig. 2. The performances of three commercially available GIMFs with core diameters of 50 μm, 62.5 μm and 100 μm, labeled GIMF50, GIMF62.5 and GIMF100 respectively, have been investigated. According to Fig. 2, a significant improvement in the transmission can be achieved employing a segment of GIMF50 of length $L_{\mathrm{MFA}} = 250$ μm between the SMF and the LMA PCF. In this case, the transmission increases from 23% up to 95.8% due to the improved mode overlap. It is important to mention that the GIMF design could be tailored to achieve perfect mode-matching with 100% transmission between the SMF and the PCF. However, several additional steps including fiber fabrication would be required which is beyond the scope of the presented investigation.

Furthermore, a complete monolithic fiber laser cavity consists of a second feedback element located at the output end of the PCF. In Fig. 3, generic monolithic fiber chains are numerically represented. Light transmission through two complete fiber laser chains SMF-PCF-SMF, without (top) and with (bottom) MFA devices has been modeled and intensity results are shown in Fig. 3. The initial poor transmission of 1064 nm light wavelength arising from the mode-field mismatch (only 5.5% corresponding to 12.5 dB loss) is significantly improved to 92% (corresponding

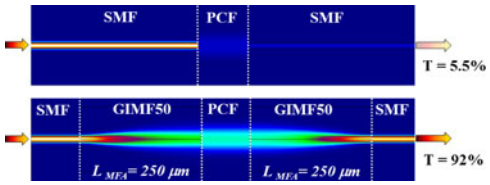

Fig. 3. Numerical simulation of 1064 nm light wavelength propagating through two fiber laser chains SMF-PCF-SMF without (top) and with (bottom) MFAs.

to 0.4 dB loss) after mode-field matching utilizing two identical MFA segments of GIMF50 with LMFA = 250 μm (see bottom Fig. 3).

IV. Experimental Demonstration

The two fiber chains presented in Fig. 3 have been fabricated and light transmission has been experimentally measured. Results can be later directly compared to numerical predictions. An easy, robust and reproducible fiber chain assembly procedure has been elaborated and individual steps are presented. The procedure is initiated by fusion splicing a piece of SMF to a piece of GIMF using a conventional arc-based splicer (FSU 995 by Ericsson). Then, a precise micrometric cleaving of a GIMF segment of length L_{MFA} is achieved using a fiber cleaver (FK 11 by PK Technology) fixed on a translation stage with micrometer steps increments and imaged with a 20x microscope objective. After imaging the splicing point between the SMF and the GIMF, the diamond blade is translated by L_{MFA} and the GIMF is cleaved with a length accuracy of ± 5 μm. The final step is to fusion splice the SMF-GIMF chain with the active LMA PCF. To simplify the splicing procedure, the PCF outer diameter (OD) has been chemically etched down from 440 μm to 240 μm, reducing the initial difference with the SMF (125 μm OD). A filament-based splicing system (GPX-3000, Vytran) with active control of the splicing parameters has been used to achieve mechanically strong splices while maintaining the air-hole structure of the PCF cladding. A microscope image of a chain SMF-GIMF-PCF fabricated following this procedure is shown in Fig. 4(a).

To measure the transmission through the two fabricated chains, a superluminescent diode, emitting 60 nm around 1050 nm, is used as the light source and is coupled into the core of one of the SMF. The transmission is measured by inserting the second SMF in an optical spectrum analyzer (OSA). The results are plotted in Fig. 4(b), comparing the transmission through a direct SMF-to-PCF coupling chain (black) with the chain employing two GIMF50 ($L_{\mathrm{MFA}} = 250$ μm) MFAs (red). We measured an overall transmission improvement of more than one order of magnitude when using an appropriate MFA. In particular, losses are reduced from -20 dB to -8 dB at 1064 nm which is close to the simulation results presented in Fig. 3 (predicting a coupling loss reduction from 12.5 dB to 0.4 dB). Thus, we experimentally demonstrated the significant increase in transmission when employing appropriate MFAs.

In both chains, the remaining $\sim$10 dB losses are attributed to splicing losses between the SIF and the PCF as it has been particularly challenging to achieve reliable good quality cleaving of the PCF facet. However, splice loss $\leq$2 dB between SIF and PCF can be achieved using highly controllable equipment [10]–[13]. In the next section, monolithic fiber laser chains employing all-fiber MFA are presented and characterized.

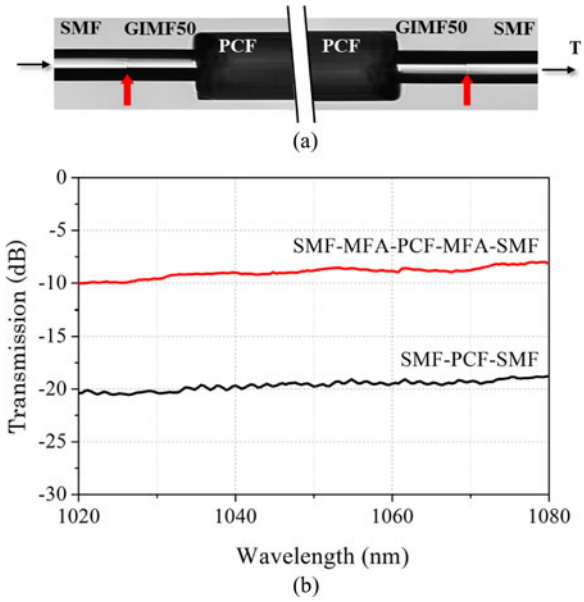

Fig. 4. (a) Microscope image of a monolithic fiber chain comprising two MFAs (GIMF 50 with $L_{\mathrm{MFA}} = 250$ μm). The splicing points between the SMF the GIMF are indicated with red arrows. (b) Light transmission measured through two fiber chains without (black) and with MFAs (red).

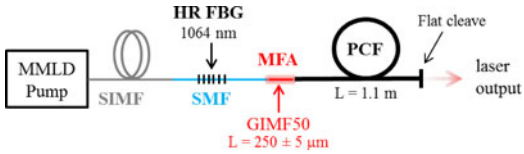

Fig. 5. Schematic of the monolithic fiber laser cavity including a 99% HR fiber Bragg grating and $\sim$4% reflective output coupler.

V. Monolithic Fiber Lasers

Two configurations of monolithic fiber lasers have been assembled. The first monolithic laser is illustrated in Fig. 5. A 974 nm wavelength multimode laser diode (MMLD) fiber coupled to a step-index multi-mode fiber (SIMF) with 105 μm core and 125 μm cladding diameter is used as the pump source. The SIMF is fusion spliced to the SMF in which a high reflector (HR) FBG has been inscribed to reflect 99% of the 1064 nm light across 14 nm FWHM bandwidth (purchased from O/E land). The FBG SMF segment is uncoated and the length is kept under 2 cm to prevent high pump scattering. The PCF cladding absorption has been measured around $\sim$15 dB/m at 974 nm pump wavelength.

Thus, the length of active PCF used in the cavity for efficient pump absorption is $\sim$1.1 m. The monolithic laser cavity is terminated by the flat cleaved output facet of the active PCF providing $\sim$4% feedback. Two chains have been fabricated, one including a MFA section ($L_{\mathrm{MFA}} = 250 \pm 5$ μm of GIMF50)

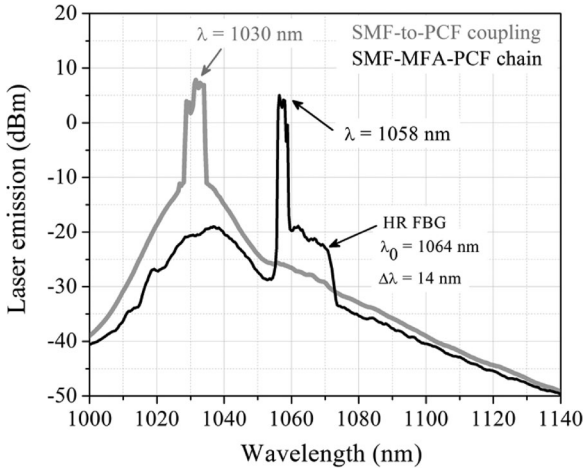

Fig. 6. Measured emission spectrum above lasing threshold through two monolithic fiber cavities with (black) and without (grey) MFA between the HR FBR and the LMA PCF.

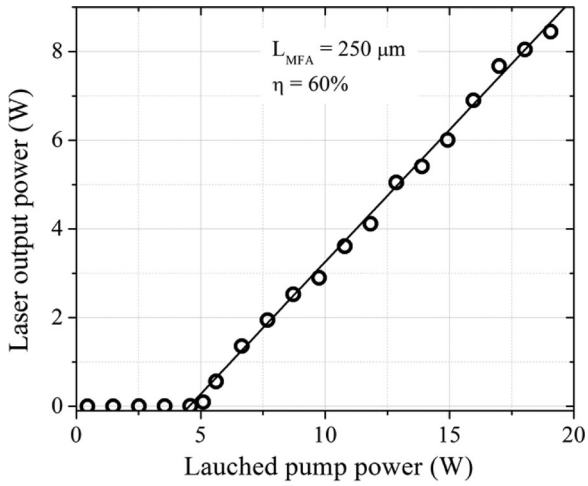

Fig. 7. Output power measured as a function of launched pump powers at 1058 nm lasing wavelength emitted by the mode-field matched laser cavity.

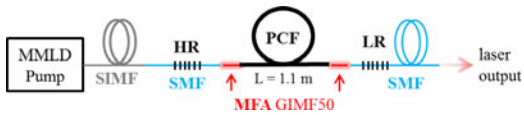

Fig. 8. Schematic of the second monolithic fiber laser cavity including two FBGs in SMF spectrally overlapping. The laser emission line-width is controlled using a narrow bandwidth LR FBG at the fiber laser output.

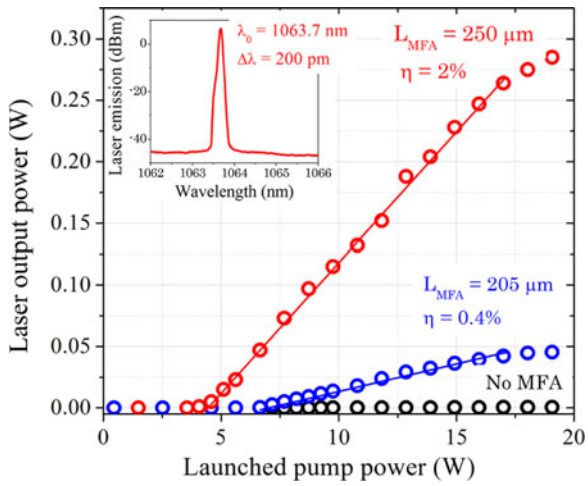

Fig. 9. Measured laser output power as launched pump power varies for three fiber laser chains: direct coupling (black), using 205 μm long MFAs pair (blue) and 250 μm long MFAs pair (red). The corresponding laser emission spectrum is depicted in insert.

between the FGB SMF and the PCF and one directly coupling the FBG SMF to the PCF. In both cases, the SMF-to-PCF spliced sections have been packaged using microscope slides to ensure mechanical strength and stability as well as low pump scattering loss along the ~2 cm long SMF-GIMF section.

For both laser cavities, the emission spectrum has been measured above threshold with an OSA and results are presented in Fig. 6. While increasing the pumping level, the chain SMF(HR FBG)-PCF, presented in grey in Fig. 6, emits a free-running laser line centered at 1030 nm, corresponding to the wavelength of maximum gain for the Yb-ions. In this configuration, the laser emission arises from parasitic reflections at the SMF-to-PCF interface which has been previously characterized with considerable losses (see Fig. 4). This laser cavity has a threshold of ~5 W and a slope efficiency of 47%.

In comparison, when pumping the chain including a MFA above threshold, a laser line centered at 1058 nm with ~30 dB signal-to-background ratio is recorded (black line in Fig. 6). This laser emission is generated from the cavity formed between the HR FBG (indicated in Fig. 6) and the 4% reflection at the PCF output. In this case, the output power has been measured as function of launched pump power. Results are plotted in Fig. 7 showing 60% of laser slope efficiency. The maximum output power of ~8 W was limited by the available pump power and by the high SIF-to-PCF splicing losses. The laser emission is stable over time. However, the laser line-width can be controlled employing spectrally narrow FBG.

A second monolithic fiber laser configuration is studied. Fig. 8 displays a schematic representation of the cavity, presenting a similar system to Fig. 5 with the addition of a low reflector (LR) FBG (30% reflective at 1063.7 nm with 0.2 nm FWHM bandwidth) written in SMF. The narrow line-width LR FBG is spliced to the output facet of the PCF to improve the laser stability over time and ensure a narrow-line laser emission. The output power has been measured for three fiber laser cavities characterized by different SMF-to-PCF coupling configurations. Results are plotted in Fig. 9. The first monolithic fiber laser chain (see black circles in Fig. 9) is assembled according to Fig. 8. However, no MFA device has been inserted at the SMF-to-PCF coupling sections.

In such a case, high cavity losses prevent any laser emission even at high pumping levels. A second fiber chain comprising two identical but non-optimized MFAs ($L_{\mathrm{MFA}} = 200$ μm of GIMF50) operates with low slope efficiency while pumping with the MMLD [blue in Fig. 5(b)]. According to our simulation (see Fig. 2), cavity losses remain high with a maximum chain transmission predicted around 56%. In comparison, a third a last

fiber chain has been assembled including two optimized MFAs segments of $L_{\mathrm{MFA}} = 250\ \mu$m of GIMF50. As the pump level increases, laser emission has been characterized performing with higher slope efficiency and output power compared to mode-mismatched laser cavities. The corresponding output spectrum is plotted in the insert of Fig. 9. We demonstrate that cavity losses arising from initial mode mismatch can be mitigated when employing two optimized MFAs. As a result, stable and narrow line-width laser emission has been measured at 1063.7 nm initiated by the LR FBG (200 pm FWHM bandwidth). In this configuration, the laser operates away from the gain maximum at 1030 nm, which limits the obtainable slope efficiency and output power. In addition, laser output performances could be further improved by reducing the remaining cavity losses, in particular through better engineering of the cleaving process.

VI. Conclusion

Here, we demonstrate monolithic fiber lasers employing all-fiber MFAs to combine an active LMA PCF and conventional FBGs in SMF. The proposed all-fiber MFA approach enables to mitigate coupling losses between two fibers (SMF and LMA PCF) presenting an initial 18-fold mode-field mismatch. We experimentally prove that the transmission through a monolithic mode-matched SMF-PCF-SMF chain can be improved by more than 10 dB. As a result, assembled monolithic fiber lasers using MFAs outperformed lasers with direct SMF-to-PCF coupling, opening the route towards the monolithic integration of LMA PCFs. It is worth emphasizing that the proposed mode-field matching method has been implemented employing only commercially available fibers and standard fiber fusion splicing equipment. It should be noted that cavity losses can be further mitigated by reducing the intra-cavity splicing losses. We believe that this MFA approach can significantly contribute to the future development of monolithic fiber laser and amplifier systems using specialty fiber designs.

References

[1] C. Jauregui, J. Limpert, and A. Tünnermann, "High power fibre lasers," *Nat. Photon.*, vol. 273, pp. 861–867, 2013.

[2] D. J. Richardson, J. Nilsson, and W. Clarkson, "High power fiber lasers: Current status and future perspectives," *J. Opt. Soc. Amer. B*, vol. 27, no. 11, pp. B63–B92, 2010.

[3] Y. Jeong, J. K. Sahu, D. N. Payne, and J. Nilsson, "Ytterbium-doped large-core fiber laser with 1.36 kW continuous-wave output power," *Opt. Exp.*, vol. 12, no. 25, pp. 6088–6092, 2004.

[4] T. Eidam, S. Hanf, E. Seise, T. V. Andersen, T. Gabler, C. Wirth, T. Schreiber, J. Limpert, and A. Tünnermann, "Femtosecond fiber CPA system emitting 830 W average output power," *Opt. Lett.*, vol. 35, no. 2, pp. 94–96, 2010.

[5] P. Yan, S. Yin, J. He, C. Fu, Y. Wang, and M. Gong, "1.1 kW Ytterbium monolithic fiber laser with assembled end-pump scheme to couple high brightness single emitters," *IEEE Phot. Technol. Lett.*, vol. 23, no. 11, pp. 697–699, Jun. 2011.

[6] C. Liu, A. Galvanauskas, V. Khitrov, B. Samson, U. Manyam, K. Tankala, and D. Machewirth, "High-power single-polarization and single-transverse-mode fiber laser with an all-fiber cavity and fiber-grating stabilized spectrum," *Opt. Lett.*, vol. 31, no. 1, pp. 17–19, 2006.

[7] A. K. Sridharan, P. Pax, M. J. Messerly, and J. W. Dawson, "High-gain photonic crystal fiber regenerative amplifier," *Opt. Lett.*, vol. 34, no. 5, pp. 608–610, 2009.

[8] O. Schmidt, C. Wirth, I. Tsybin, T. Schreiber, R. Eberhardt, J. Limpert, and A. Tünnermann, "Average power of 1.1 kW from spectrally combined, fiber-amplified, nanosecond-pulsed sources," *Opt. Lett.*, vol. 34, no. 10, pp. 1567–1569, 2009.

[9] S. Klingebiel, F. Röser, B. Ortaç, J. Limpert, and A. Tünnermann, "Spectral beam combining of Yb-doped fiber lasers with high efficiency," *J. Opt. Soc. Amer. B*, vol. 24, no. 8, pp. 1716–1720, 2007.

[10] P. J. Bennett, T. M. Monro, and D. J. Richardson, "Toward practical holey fiber technology: Fabrication, splicing, modeling and characterization," *Opt. Lett.*, vol. 24, no. 17, pp. 1203–1205, 1999.

[11] B. Bourliaguet, C. Paré, F. Emond, and A. Croteau, "Microstructured fiber splicing," *Opt. Exp.*, vol. 11, no. 25, pp. 3412–3417, 2003.

[12] L. Xiao, M. S. Demokan, W. Jin, Y. Wang, and C. Zhao, "Fusion splicing photonic-crystal fibers and conventional single-mode fibers: Microhole collapse effect," *J. Lightw. Tecnol.*, vol. 24, no. 11, pp. 3563–3574, Nov. 2007.

[13] L. R. Jaroszewicz, M. Murawski, T. Nasilowski, K. Stasiewicz, P. Marc, M. Szymanski, P. Mergo, W. Urbanczyk, F. Berghmans, and H. Thienpont, "Low-loss patch cords by effective splicing of various photonic crystal fibers with standard single mode fiber," *J. Lightw. Technol.*, vol. 29, no. 19, pp. 2940–2946, Oct. 2011.

[14] J. C. Chong, M. K. Rao, Y. Zhu, and P. Shum, "An effective splicing method on photonic crystal fiber using CO2 laser," *IEEE Photon. Technol. Lett.*, vol. 15, no. 7, pp. 942–944, Jul. 2003.

[15] D. Marcuse, "Loss analysis of single-mode fiber splices," *Bell Syst. Tech. J.*, vol. 56, no. 16, pp. 703–718, 1977.

[16] J. Liu, T. Cheng, Y. Yeo, Y. Wang, L. Xue, Z. Xu, and D. Wang, "Light beam coupling between standard single mode fivers and highly nonlinear photonic crystal fibers based on the fused biconical tapering technique," *Opt. Exp.*, vol. 17, no. 5, pp. 3115–3123, 2009.

[17] Z. Chen, X. Xi, W. Zhang, J. Hou, and Z. Jiang, "Low-loss fusion splicing photonic crystal fibers and double cladding fibers by controlled hole collapse and tapering," *J. Lightw. Technol.*, vol. 29, no. 24, pp. 3744–3747, Dec. 2011.

[18] T. Zhu, F. Xiao, L. Xu, M. Liu, M. Deng, and K. S. Chiang, "Pressure-assisted low-loss fusion splicing between photonic crystal fiber and single-mode fiber," *Opt. Exp.*, vol. 20, no. 22, pp. 24465–24471, 2012.

[19] A. D. Yablon and R. T. Bise, "Low-loss high-strength microstructured fiber fusion splices using GRIN fiber lenses," *IEEE Photon. Technol. Lett.*, vol. 17, no. 1, pp. 118–120, Jan. 2005.

[20] B. G. Ward, D. L. Sipes Jr., and J. D. Tafoya, "A monolithic pump signal multiplexer for air-clad photonic crystal fiber amplifier," *Proc. SPIE*, vol. 7580, p. 75801C, 2010.

[21] J. Canning, N. Groothoff, K. Cook, C. Martelli, A. Pohl, J. Holdsworth, S. Bandyopadhyay, and M. Stevenson, "Gratings in structured optical fibers," *Laser Chem.*, vol. 2008, no. 239417, p. 19, 2008.

[22] A. Mafi, P. Hofmann, C. J. Salvin, and A. Schülzgen, "Low-loss coupling between two singl-mode optical fibers with different mode-field diameters using a gradded-index multimode optical fiber," *Opt. Lett.*, vol. 36, no. 18, pp. 3596–3598, 2011.

[23] P. Hofmann, A. Mafi, C. Jollivet, T. Tiess, N. Peyghambarian, and A. Schülzgen, "Detailed investigation of mode-field adapters utilizing multimode-interference in graded index fibers," *J. Lighw. Technol.*, vol. 30, no. 14, pp. 2289–2298, Jul. 2012.

Clémence Jollivet received the B.S. degree in physics and chemistry and the M.S. degree in physics from the University of Bordeaux 1, Bordeaux, France in 2007 and 2009, respectively. She received the M.S. degree in optical sciences in 2012 from CREOL, the College of Optics and Photonics, University of Central Florida in Orlando (USA). She is currently working toward the Ph.D. degree in optics from CREOL. Her research interests include design, fabrication, and characterization of specialty fibers, in particular advanced characterization techniques for modal analysis as well as development of novel specialty fiber lasers and devices. She is a member of the International Society for Optics and Photonics SPIE and of the Optical Society.

Julie Guer received the B.S. degree in physics in 2012 from the University of Tours, France. She is currently working toward the M.S. degree in physical instrumentation at the University of Bordeaux 1, France. His topics include design, use and sale of physical instruments, in particular of photonic instruments. During her studies, she spent one semester in CREOL, the College of Optics and Photonics in the University of Central Florida (USA).

Peter Hofmann received the B.S. degree in optoelectronics from the University of Aalen, Germany, in 2006. He received the M.S. and Ph.D. degrees in optical sciences in 2011 and 2012, both from the College of Optical Sciences, University of Arizona in Tucson. He has several years of experience in the laser industry. Until fall 2013 he worked as a Research Scientist at the College of Optics and Photonics CREOL. His research interests include new material fibers, fiber, and solid state lasers. Recently, he joined Time-Bandwidth Products AG in Zurich Switzerland.

Axel Schülzgen received the Ph.D. degree in physics from Humboldt-University of Berlin, Germany, in 1992. Since 2009, he has been a Professor of Optics at CREOL, The College of Optics and Photonics, University of Central Florida in Orlando. Prior to joining CREOL he was a faculty member at The College of Optical Sciences, University of Arizona in Tucson. His current research interests include optical fiber devices, components, materials, and structures with applications in fiber laser systems and fiber optic sensing. Dr. Schulzgen is a member of the Optical Society of America, the International Society for Optics and Photonics SPIE, and the German Physical Society. He currently serves as the Topical Editor of *Applied Optics*, a journal of the Optical Society of America.